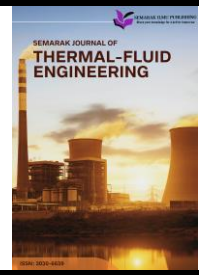




Semarak Journal of Thermal-Fluid Engineering

Journal homepage:
<https://semarakilmu.my/index.php/sjotfe/index>
ISSN: 3030-6639



Comparative Study of Internal Flow Dynamics Using CFD (Y-Junction Pipe)

Muhammad Dzul Imran Ismail^{1,*}

¹ Department of Mechanical Engineering and Manufacturing, Fakulti Kejuruteraan Mekanikal dan Pembuatan, Universiti Tun Hussein Onn Malaysia, 86400 Parit Raja, Johor Darul Ta'zim Malaysia

ARTICLE INFO

Article history:

Received 10 June 2025
Received in revised form 19 July 2025
Accepted 31 July 2025
Available online 29 September 2025

Keywords:

Y-junction pipe; computational fluid dynamics; pressure and velocity distribution

ABSTRACT

This paper compares the flow behaviour inside Y- junction pipe through a CFD based ANSYS Fluent analysis. The study investigates the influence of pipe diameter (0.1 m and 0.2 m) and inlet velocity (0.297 m/s, 0.397 m/s and 0.497 m/s) on the flow dynamics, pressure distribution and velocity profiles. The simulations are performed by solving the steady Navier–Stokes equations for both incompressible, using the finite volume method. The effects of geometric and velocity changes on flow features, including secondary flows, flow separations and pressure drops, are investigated from which significant differences are observed. These are useful results to demonstrate the internal flow feature of Y-junction pipes, and to optimize design of transporting fluid systems.

1. Introduction

Pipeline internal flow is an essential element of fluids transmission system which extensively exist in a variety of engineering situations such as water distribution network, heat exchanger as well as chemical-processing equipment. The knowledge of flow characteristics is particularly important in case of turbulent flow for optimal operation of the system and to prevent system failures. Computational Fluid Dynamics (CFD) offers capabilities to visualize and analyse intricate flow patterns, enabling engineers to test scenarios with a variety of conditions without conducting complex physical testing. CFD has allowed a better understanding of flow mixing and particle distribution at Y-junctions as it is especially important in the fields of chemical reactors or water distribution networks because it can help in the calculation of the precise amount of chemicals or waste products in the reactor or network. The effect of junction geometry and inlet flow conditions on mixing efficiency and RTDs, which has been shown by various reports studies, are strongly affected by the flow characteristic [1,2].

Moreover, recent developments in CFD tools made it possible to more accurately predict erosion and mechanical stresses in junctions to design more durable piping system [3]. Such flow phenomena are generally characterised by the existence of low pressures zones and high pressures gradients

* Corresponding author.

E-mail address: CD210013@student.uthm.edu.my

<https://doi.org/10.37934/sjotfe.6.1.4256a>

that are of utmost importance for the optimal design of piping systems and hydraulic systems in a wide range of engineering fields [4]. The comparison of internal flows is a challenging research question and needs attention, especially in Y-junctions pipe to solve the fluidic behaviours in complex geometries. A key topic is the loss that occurs due to continuity of flow and generation of turbulence at junctions. Gajbhiye *et al.*, [1] discussed the effect of pipe fittings on the flow phenomenon, indicating the importance of correct modelling in the prediction of pressure loss and to optimize system design. It is more essential because it is presented that the energy loss during flow convergence and divergence at junctions might affect hydraulic calculation substantially [5]. There are a few studies that identify the complexities of numerically simulating flow in Y-junction pipes.

Ferreira *et al.*, [6] showed that the elbow configuration has a strong influence on pump inlet flow conditions, which govern the overall system efficiency. These results then lead to certain questions of how such similar geometry of Y-junctions influence flow stability and pressure distribution. In line with this, Gajbhiye *et al.*, [1] found that turbulence and separation contribute to pressure losses in pipe fittings and hence require reliable computational tools to estimate these losses in complex junctions. Additionally, Decaix *et al.*, [7] studied hydraulic short circuits in junctions and showed that poorly designed junctions could induce noticeable discrepancies in the discharge rates of connected pipes, which may result in ineffective operation of hydropower systems. This observation underscores the need for more detailed characterization and modelling of junctions for design considerations, given that design errors can result in large variations of power and operational performance. The importance of accurate prediction to the temperature fluctuations and various models for the turbulence flow are the part of the study as well.

Lopez-Santana *et al.*, [8] emphasise the significance of benchmarking the experimental techniques against CFD approaches to estimate the accuracy of the turbulent flow predictions and validate the computational results with existing empirical data. This comparison approach is essential in the development the predictive model of flow condition in Y-junctions with characteristics of high reliability. Therefore, the fundamental issue taken into consideration in this study is the lack of knowledge of the detailed internal flow patterns within a Y-junction pipe. In this work, we employ sophisticated CFD methods to examine the flow features such as velocity, pressure and turbulence kinetic energy under a wide range of operating conditions for the purpose of offering fundamental guidelines for optimizing the design and improving the efficiency of operation in question engineering applications. However, as vital as these junctions are, studies had earlier revealed the challenges of accurately capturing the intricate flow boundary conditions at these junctions. For example, Vigolo *et al.*, [9] who discussed the trapping of particles due to fluid dynamics at T-junctions, showed how inertia and alterations of the flow directions develop elaborate flow regimes of importance in the proper functioning of piping networks.

Similarly, Doi *et al.*, [10] found that the fluid dynamics when crossing junctions are geometrical-dependent, with sharp junctions having different flow features from more gradual transitions. The forming of these flow features is important to recognize to avoid losses and help design the optimal hydraulic performance, for instance in the context of hydropower, see analysis on hydraulic short-circuits through junctions [7]. The work of Marušić-Paloka, [11] served to further emphasize the need to study fluid flow interactions at junctions, detailing how different flow systems will affect the efficiency and reliability of systems. It is also worth mentioning that previous works have stressed the role of the turbulence models, especially in Y-junctions, on the need to give a correct approximation of the flow in real flow cases. Gajbhiye *et al.*, [1] highlighted these discrepancies in pressure drop predictions owing to different computational methods, wherein a proper CFD methodology is vital.

Furthermore, complex junction interactions may cause large differences of the discharges of connecting pipes, which can eventually destabilize the systems, especially in the case of hydraulic short-circuits [12]. The effects of flow rate ratios on loss reduction of T-junction pipe have been investigated, which the results show the momentous dependence of the separation and vortex on the total flow resistance [13]. Analytical and numerical analyses in prior work suggest that the complex flow field near Y-junction require careful consideration in terms the morphology. For instance, Raschi *et al.*, [14] performed CFD simulations to study reactor fluidization hydrodynamics and paid attention to the influence of the geometrical conformation on the flow profiles. These findings highlight the role of geometry on flow characterization and the necessity to simulate accurately the fluid dynamics in junction geometries. Another example of CFD being used to model complex flow behaviour is the study by Decaix *et al.*, [12]. In this work, CFD simulations of hydraulic short-circuit phenomena at junctions were able to provide explanations for what were previously deemed anomalous findings [15]. Such methods could be used to help guide design guidelines of Y-junctions to avoid the problem of imbalance flow distribution.

In order to process the effect of the fluid flow on the system performance, advanced computational methods are required to be performed. For example, Miyazaki *et al.*, [16] proved the applicability of CFD in medicine, presenting the method's cross-disciplinarity to characterize turbulent flows. Compared to this, study of flow through Y-junction pipes has been reported in various research of CFD since it can visualize the flow behaviour such as flow pattern, mixing zone and pressure lose. Based on Miyazaki *et al.*, [16], simulations with CFD show the existence of the vortexes in the Y-junction and their effect on the efficiency of the system. In addition, the work of Hardy *et al.*, [17] showed that the geometry of the bifurcation, in terms of angle between branches, affected velocity and pressure distributions. Zhang *et al.*, [18] determined that the k- ϵ model gives good predictions for complex branched pipe flows. In addition, the work of Yin *et al.*, [19] was used as a comparison for CFD results in three-dimensional flows in Y-pipes. Finally, Boz *et al.*, [20] demonstrated that a refined mesh in the junction also raises CFD accuracy by providing a better resolution of the recirculation zone.

In the present work, CFD is used to examine the influence of different pipe diameters and flow rates on the internal flow field of a straight pipe. Three different pipe diameters 0.1 m, and 0.2 m are considered for three flow velocities 0.297 m/s, 0.397 m/s and 0.497 m/s. A straight pipe geometry is chosen to study the impact of flow parameters in a controlled manner, without any additional complex changes in geometry such as bends or shapes. In this simulation, three essentials turbulent internal flow properties including velocity distribution, static pressure and turbulence kinetic energy are simulated and analysed. Velocity profiles are indicative of how uniformly the fluid flows in the pipe, pressure distributions contribute to the identification of possible losses and gains in energy, and turbulence kinetic energy gives information on the level of turbulence, as well as on energy content fluctuation in the flow. By reviewing these factors for all diameter-velocity pairs, a thorough understanding can also be sought as to how geometric and operational considerations impinge on internal turbulent flow. The results of this study can provide valuable references for the optimal design of the pipeline and predicting the flow performance of engineering systems.

2. Methodology

2.1 Geometry Construction

In this study, two computational models representing straight pipe sections were developed to analyse internal flow dynamics using CFD as shown in Figure 1. The first model (diameter 1) had a length of 1.0 m and a diameter of 0.1 m, while the second model (diameter 2) also had a length of

1.0 m but with a larger diameter of 0.2 m. These geometries were designed using ANSYS Design Modeler to ensure accurate representation of the pipe flow domain. The aim was to observe how variations in pipe diameter influence velocity, pressure, and turbulence characteristics under identical inlet conditions. The geometry was kept simple, with no branching or bends, to isolate the effects of diameter alone.

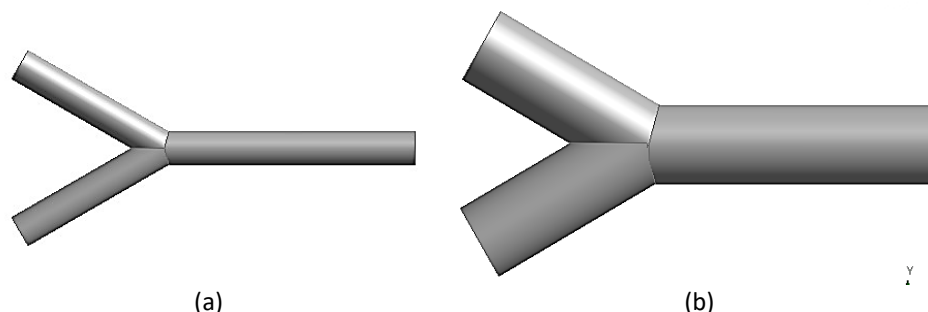


Fig. 1. Geometry model of the Y-pipeline (a) Diameter 0.1 m (b) Diameter 0.2 m

2.2 Mesh Generation and Grid Independent Test

The meshing process was carried out using ANSYS Meshing, employing a structured tetrahedral mesh with inflation layers applied near the wall surfaces to capture boundary layer effects more accurately. To ensure mesh independence, three different element sizes were tested: 0.02 m (Mesh 1), 0.019 m (Mesh 2), and 0.018 m (Mesh 3). Simulation results, including velocity and pressure distribution, were compared across these three mesh cases. The comparison showed that the results between Mesh 2 and Mesh 3 were nearly identical, indicating that further mesh refinement beyond 0.019 m did not yield significant accuracy improvements. Hence, Mesh 2 was selected for all final simulations as it provided a good balance between accuracy and computational efficiency. This is all summarised in Table 1.

Table 1

Grid independence test (GIT)

| Diameter (m) | Element size (m) |
|--------------|------------------|
| 0.01 | 0.02 |
| | 0.019 |
| | 0.018 |
| 0.02 | 0.02 |
| | 0.019 |
| | 0.018 |

2.3 Boundary Condition and Flow Parameter

The simulations were conducted under turbulent flow conditions for water at room temperature. At the inlet, three different uniform velocity values were applied: 0.297 m/s, 0.397 m/s, and 0.497 m/s. These inlet velocities were tested for both pipe diameter models to assess the combined impact of velocity and diameter on internal flow behaviour. The outlets were set as pressure outlets with zero-gauge pressure, while the pipe walls were defined as no-slip boundaries. The working fluid was assumed incompressible with constant density and viscosity. The standard k- ϵ turbulence model was selected due to its reliability and widespread application in internal pipe flow simulations. This is all summarised in Table 2 and Table 3.

Table 2

Boundary condition of straight line

| Boundary Type | Location | Condition type | Value |
|---------------|-----------------|-----------------|---------------------------------------|
| Inlet | Pipe entrance | Velocity inlet | 0.297 m/s, 0.397 m/s, 0.497 m/s |
| Outlet | Pipe exit | Pressure outlet | 0 Pa (gauge pressure) |
| Wall | Pipe inner wall | No-slip wall | Velocity = 0 m/s at the surface |

Table 3

Flow parameters

| Diameter (m) | Velocity 1 (ms^{-1}) | Velocity 2 (ms^{-1}) | Velocity 3 (ms^{-1}) | Outlet | Turbulence intensity | Turbulence model |
|--------------|---------------------------------|---------------------------------|---------------------------------|--------|----------------------|------------------|
| 0.1 | 0.297 | 0.397 | 0.497 | 0 | 5% | $k - \omega$ |
| 0.2 | 0.297 | 0.397 | 0.497 | 0 | 5% | $k - \omega$ |

2.4 Post-Processing and Flow Analysis Parameters

Post-processing was carried out using ANSYS Fluent to analyse the internal flow characteristics. Key parameters extracted included velocity magnitude, turbulence kinetic energy (TKE), and pressure. Contour plots, vector flow diagrams, and line graphs were generated to visualize the flow development and identify changes in flow behaviour due to variations in diameter and inlet velocity. Additionally, cross-sectional profiles were used to examine the uniformity of flow and detect any signs of secondary motion or recirculation zones.

3. Results

3.1 Grid Independence Test (GIT)

The meshing process was carried out using ANSYS Meshing, employing a structured tetrahedral mesh with inflation layers applied near the wall surfaces to capture boundary layer effects more accurately. To ensure mesh independence, three different element sizes were tested: 0.02 m (Mesh 1), 0.019 m (Mesh 2), and 0.018m (Mesh 3). Simulation results, including velocity and pressure distribution, were compared across these three mesh cases. The comparison showed that the results between Mesh 2 and Mesh 3 were nearly identical, indicating that further mesh refinement beyond 0.019 m did not yield significant accuracy improvements as shown in Table 4. Hence, Mesh 2 was selected for all final simulations as it provided a good balance between accuracy and computational efficiency.

Table 4

Value of element sizing

| Diameter (m) | Element size (m) | Nodes |
|--------------|------------------|--------|
| 0.01 | 0.02 | 22504 |
| | 0.019 | 26629 |
| | 0.018 | 31074 |
| 0.02 | 0.02 | 81928 |
| | 0.019 | 95089 |
| | 0.018 | 111102 |

In the current study, it is chosen to consider two different pipe diameters 0.1 m and 0.2 m. In each case, three different mesh densities are defined by changing the value of element sizing which,

in essence, defines how fine or how coarse the mesh can be as shown in Table 4. For the 0.1 m diameter pipe, the largest essentially, the coarsest mesh with the element sizing 0.02m, results in 22,504 elements. When the sizing decrease to 0.019m and 0.018m, the number of elements grows to 26,629 and 31,074, respectively. Such growth occurs because the existence of more elements allows simulation to more fully grasp the changes that take place during the flow, especially near the walls and near the intersections when most changes take place.

For the 0.2 m diameter pipe, the trends are similar but occur on a larger scale. Thus, at the largest element size of 0.02m, there are 81,928 elements, and at the smallest of 0.018m, there are 111,102-element mesh. More elements are needed because the greater size of a pipe means more volume and more outer surfaces that need to be covered, which requires more elements to make the mesh similar in detail. Figure 2 is provided to compare the visual image of the Y-junction pipe under different mesh densities. Fibrous reduction in the element size makes the mesh more detailed to ensure the higher level of the CFD simulation accuracy. Nonetheless, this directly increases the computational requirement because more elements equal more calculations for the computer. The CFD choice to lower the element size should always balance between higher quality and effort a crucial balance in any CFD study.

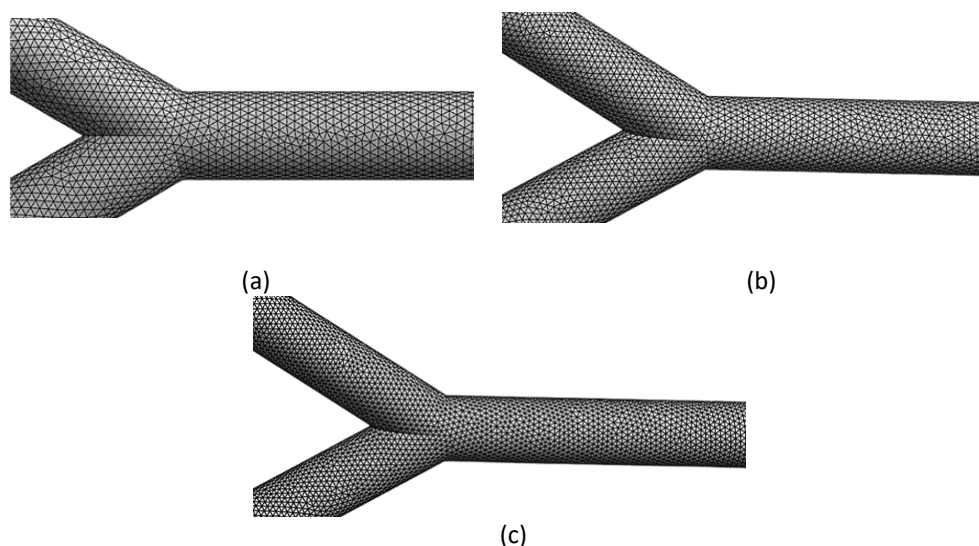


Fig. 2. Meshing element size (a) 0.02 m (b) 0.019 m (c) 0.018 m

3.2 Graph for Key Parameters

3.2.1 Fluid velocity

For the 0.1 m diameter pipe, you are starting just above 0.5 m/s at the inlet, as shown in Figure 3. As the fluid proceeds down the pipe, the velocity ramps up rapidly in the first 0.2 m. Beyond that initial climb, the rise levels off and the velocity approaches a constant value, about 0.66 m per second, at the far end of the pipe. This pattern indicates the fluid initially accelerates rapidly and then enters a steady flow as it moves downstream. Similarly, the 0.2 m pipe shows the same trend, with a few distinctions. The initial speed is also slightly higher, just above 0.5 m/s, but the rate of acceleration is a bit less dramatic. The fluid stops accelerating after a while and stabilizes at about 0.62 m/s. It is an indication that faster stabilization is attained for the wider pipe however, the maximum velocity is a bit smaller compared to the narrower pipe.

In general, these findings demonstrate the impact of the pipe diameter on the fluid velocity evolution. In either case the flow becomes more stable and uniform further downstream of the

entrance, but the narrower pipe permits a higher flow speed at the end and the wider pipe stabilizes the flow sooner.

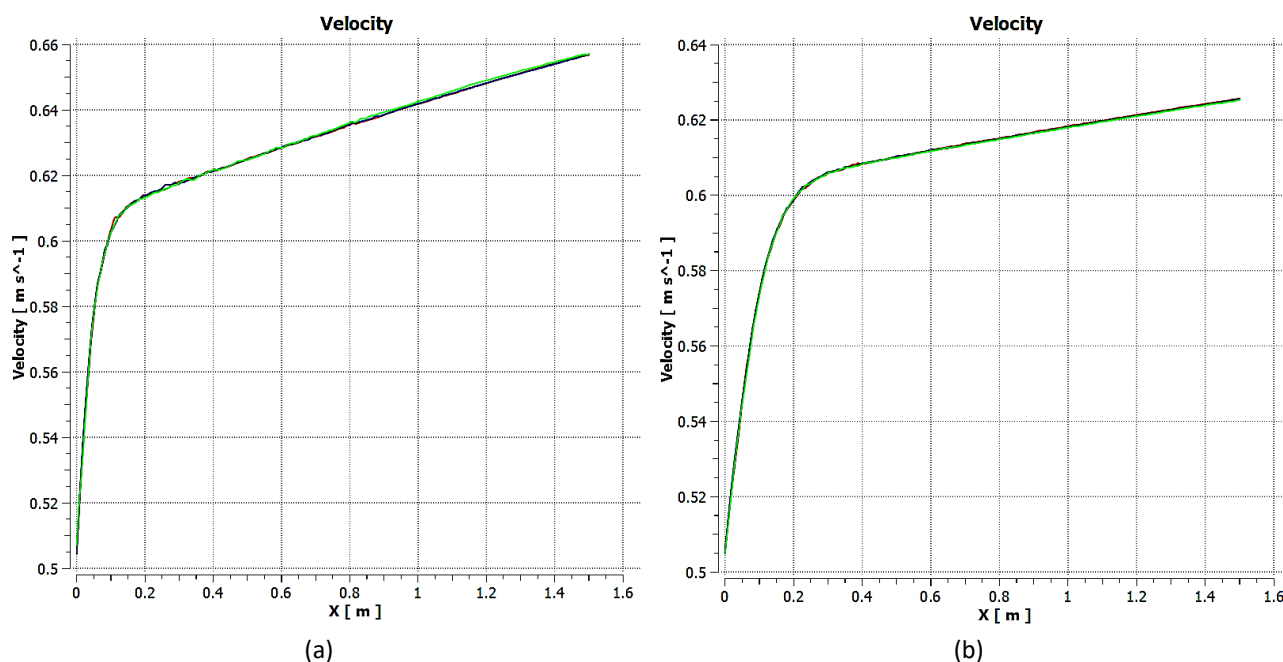


Fig. 3. Fluid velocity graph (a) Diameter 0.01 m (b) Diameter 0.02 m

3.2.2 Turbulent kinetic energy

For the narrower tube (0.1 m in diameter) the value of the turbulent kinetic energy at the first-time step is quite high, ranging between $0.00035 \text{ m}^2/\text{s}^2$ to $0.0004 \text{ m}^2/\text{s}^2$ near the pipe inlet, as shown in Figure 4. In the early region, the curves of the two numbers for the three different simulations or measurement series exhibit small fluctuations which means the turbulence has not yet adapted to the geometry of the pipe. Turbulent energy also starts decreasing after the first 0.1 m to 0.2 m down the pipe. At around the meter scale, the turbulence has decayed significantly, dropping to values of around $0.0001 \text{ m}^2/\text{s}^2$. This means that the chaotic motion of the fluid is relaxing toward calm as it moves away from the entrance, arriving at a more ordered state.

In the larger 0.2 m diameter pipe, we observe a comparable pattern, although with some slight differences. The initial turbulent kinetic energy is only a bit smaller, slightly below $0.0002 \text{ m}^2/\text{s}^2$. On the narrower pipe, there are also some ripples further back in the chart but not pronounced. With the advancing flow the decay of turbulence is less abrupt and complete as it is evident by the convergence of all three curves as flow evolves. The energy of this turbulence has again mostly dissipated and by the time the fluid has travelled to the other end of the pipe the turbulent energy is almost as low as that of the smaller pipe.

In general, the graph shows that turbulence is maximized at the spot where the fluid enters the pipe, especially in the narrower pipe where energy and the chaos are heightened. As the liquid moves further through the tube, the turbulence naturally diminishes, and the flow seems calmer and more regular. The larger pipe appears to make the fluid quiet down more rapidly with initially less violent and a smoother progression to steady flow.

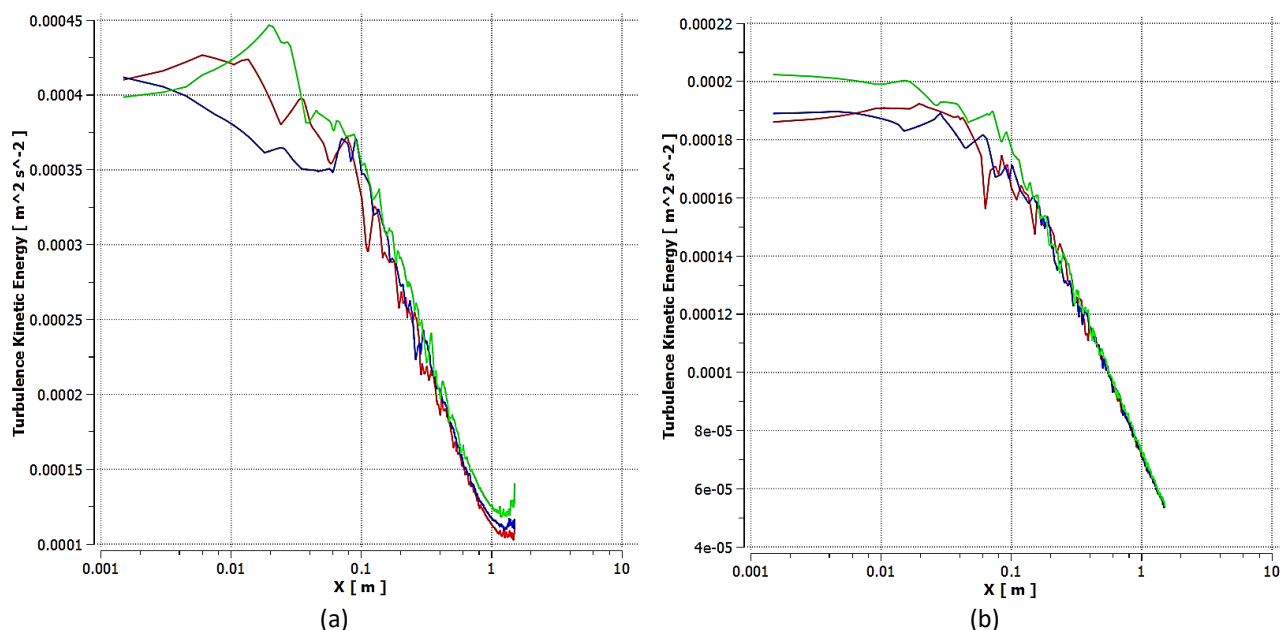


Fig. 4. Graph for turbulence kinetic energy (a) Diameter 0.01 m (b) Diameter 0.02 m

3.2.3 Pressure

Looking at the pipe with a 0.1 m diameter at the first chart a, the pressure is already quite high just above 80 Pa right at the entrance. However, almost immediately it experiences a sharp and steep decline within the first 0.2 m of the pipe. This suggests significant resistance and energy loss as the fluid enters and starts to flow through the narrower space. While afterward, it continues to decline, it does so much milder and gentler as the fluid moves further downstream. By the time it reaches the end of the 1.6 m pipe, the pressure is nearly zero. It is likely that most of the pressure loss occurs right at the beginning, followed by stabilization as the flow continues. When it comes to the one with a 0.2 m diameter, it tells a similar but slightly different story.

Here, the pressure at the entrance is lower to begin with just above 65 Pa. It starts to decline steeply at the same first 0.2m mark but is not as sharp as in the narrower pipe. After that initial steep decline, it continues for a much longer length steadily, also approaching zero by the end of the pipe. It is clear from Figure 5(a) and Figure 5(b) that the narrower pipe 0.1 m starts with a higher pressure at the entrance and loses it much quicker while the wider pipe 0.2 m starts with a lower pressure and experiences a less sharp drop. In both cases, most of the pressure loss is concentrated right at the beginning then it went by a slow, steady decline.

As water forced through two inlets with different diameter, the narrow diameter makes it difficult to go through initially, so the pressure drops rapidly as soon as it starts to flow in. The wider one is less restrictive, so while the pressure drop is still significant, it is not nearly as sharp. In both cases, however, once it starts flowing it flows smoothly, and pressure continues to drop slowly, steadily, until the fluid exits. These results once again demonstrate how pipe diameter affects pressure loss in internal flows: the narrower the pipe, the higher initial pressure and sharper drop with low downstream; and the wider it, the equation is the opposite due to a lack of restriction. This is extremely important when it comes to planning piping systems since they must be designed to accommodate high-pressure systems.

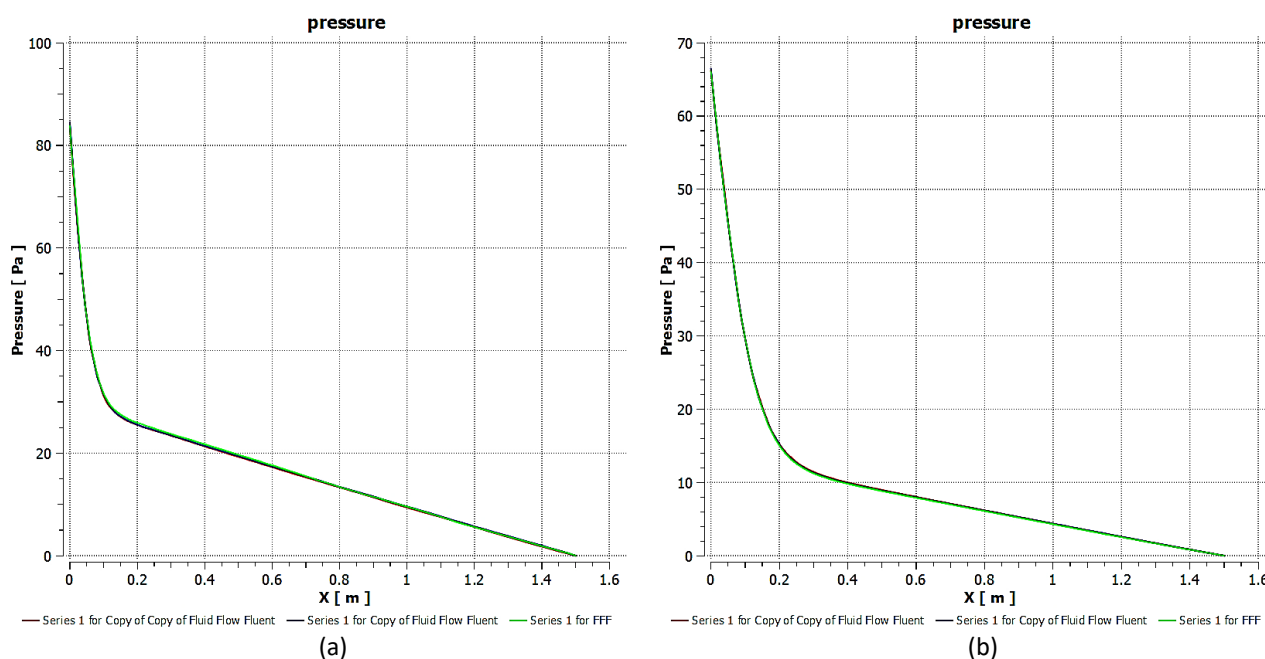


Fig. 5. Graph for pressure (a) Diameter 0.01 m. (b) Diameter 0.02 m

3.3 Contour Distribution

3.3.1 Fluid velocity

In Figure 6(a), the velocity distribution for a single configuration is shown. The main offtake is nicely progressive from blue to green to yellow, presumably indicating that as the liquid enters, it does so more slowly, then accelerates as it continues downstream. This colour changes at the branch reflects a change in velocity redistribution. One of the fluid streams slows as it moves into the branches, while the main leg still carries the fastest flow, represented by the red streak. A similar pattern is seen for Figure 6(b) but with some slight differences (likely due to increased diameter or changes in flow conditions). The velocity in the main pipe continues to be high but the branches are working more with longer regions of green and yellow. This implies that, for a bigger diameter, the fluid can go at much higher speed when it is being divided, therefore the energy losses at the junction are lower.

In Figure 6(c), the main pipe is mostly red, which shows that the fluid is moving fastest along the centre line. Some of that energy is depleted as the flow approaches the Y-junction, and the fluid decelerates in the branches a tendency represented by the shift to green and blue. Such a pattern is common at junctions (local divergence), changing flow into a positive extra kinetic energy source and velocity reduction. The velocity contours visually show how the profile of the pipe and the junction affect the flow pattern. Max velocities are carried in the primary leg of the pipe, particularly the smaller pipe, while the secondary pipes slow down as the flow divides and changes direction. This becomes essential for the engineers so that they can be aware of where in the pipeline they could potentially face a problem such as erosion, pressure drop, flow separation and optimize the design of pipes that can efficiently transport the fluid.

In Figure 7(a), one can observe that the incoming flow into the main pipe flows towards the junction. Velocity is moderate, mostly in the green and yellow area, demonstrating a consistent but not a very fast flow. The fluid slows down as it churns round the split, particularly amongst the branches, where it is a lovely blue and green. This means that the flow is losing energy as it bifurcates, and the branches are taking the fluid away at a more leisurely speed. Meanwhile, in Figure 7(b), the main pipe also shows wider yellow and even some orange above it, signifying a faster fluid

velocity than in Figure 7(a). The velocity is still higher when the flow arrives and passes through the junction, and the branches look more green and yellow. In other words, in the case of some fronds, the fluid holds onto more of its speed as it splits, and the branches can transport a faster flow.

Finally, in Figure 7(c), the main pipe is mostly bright red and orange over the main pipe and showing that the fluid is in the maximum speed. When passing through the branches, the fluid is still fast, shown by the yellow and green area. Flow here is unsolved for the most part, giving it plenty of energy and force as it splits at the fork. The simulation in general demonstrate how different flow rate regime or PDMS simulation conditions can influence the distribution of velocities in the Y-junction. When the fluid moves faster through the main pipe, the speed of the fluid in the branches after the split increases. This information is important for engineers and designers, who can use it to estimate how different operating conditions will affect the performance and efficiency of pipe systems, particularly in complex geometries such as T-junctions where the flow can have unpredictable behaviour.

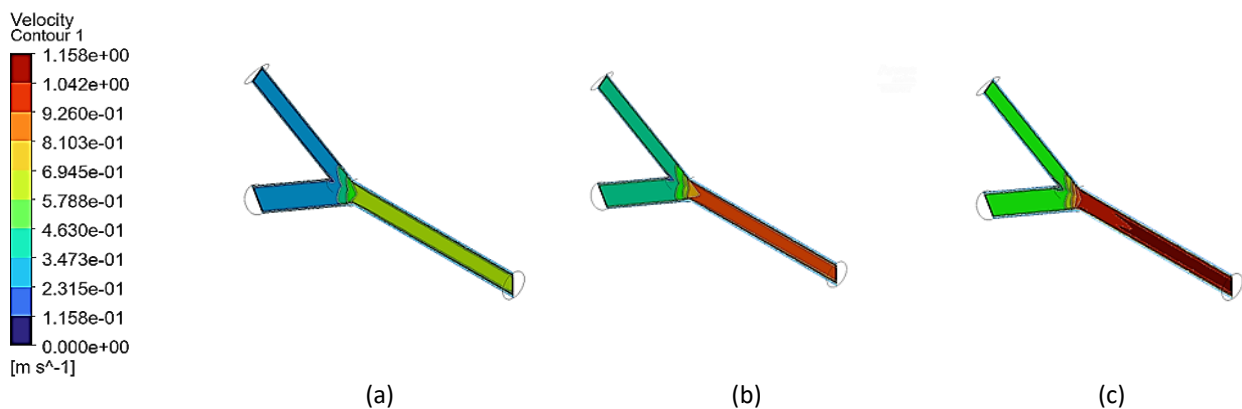


Fig. 6. Velocity distribution for Y Junction pipe of diameter 0.1 m (a) Inlet velocity = 0.297 m/s (b) Inlet velocity = 0.397 m/s (c) Inlet velocity = 0.497 m/s

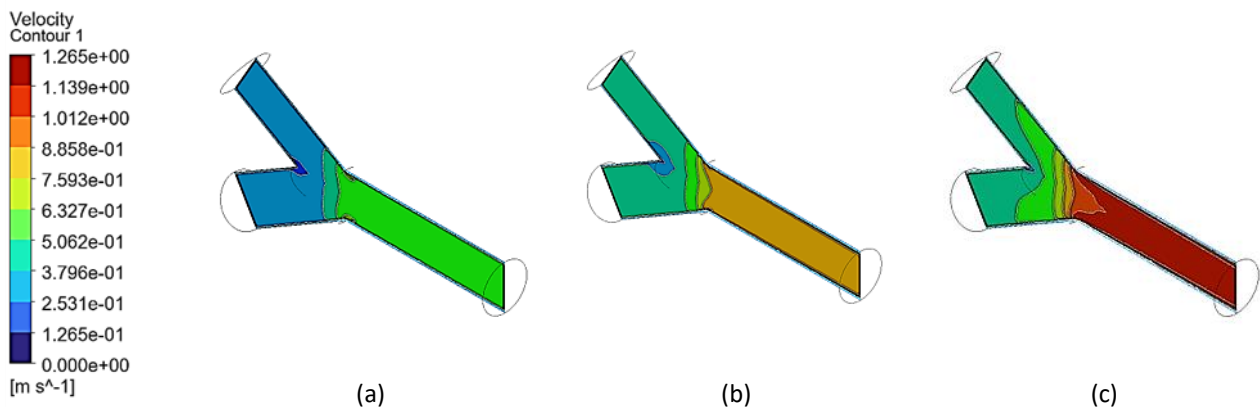


Fig. 7. Velocity distribution for Y Junction pipe of diameter 0.2 m (a) Inlet velocity = 0.297 m/s (b) Inlet velocity = 0.397 m/s (c) Inlet velocity = 0.497 m/s

3.3.2 Turbulent Kinetic Energy

If we look back at these three images in Figure 8, we can see that each one tells a part of the full story regarding how turbulence presents itself as a fluid flow through a Y-junction pipe of 0.1 m in diameter. The colours on each pipe, from deep blue to bright red, reflect the intensity of the turbulent kinetic energy, with blue representing the calmer regions and red showing the most energetic areas

of turbulence. First, in Figure 8(a), we see that most of the pipe is characterized by dark blue, meaning that the turbulent kinetic energy is quite low for most of this system. We can see a thin line of a lighter tone of colour around the pipe wall and branches, which indicates that there's a small region where there might be turbulence as well, however, it's hugging the wall and is incredibly weak.

In Figure 8(b), we see a similar case except that the thin line around the pipe wall is a little bit more pronounced, and it continues further down the line inside the pipe than before. This thinner line changes its colour slightly towards green and yellow, indicating that the turbulent kinetic energy is slightly higher than in Figure 8(a). This implies that under these conditions, this system is slightly more agitated, especially where the flow is affected by the pipe-wall interaction.

Finally, in Figure 8(c), the thin line near the pipe wall is developed and clearer, extending all the way both from the main inlet, through the junction, and into the branches. The line is much brighter around this image, as it gets to move towards yellow and even light orange shades. This indicates that the turbulent kinetic energy is higher, meaning that the fluid is under more chaotic, energetic flow conditions, especially where the flow is splitting in the Y-junction. In all three figures, the core of the pipe remains dark blue, indicating that the flow is relatively calm but turbulent areas are present near the walls. This is typically the case with pipe flows since the walls generate the most turbulence due to the interaction and Y-junctions because the flow is encountering significant changes in direction.

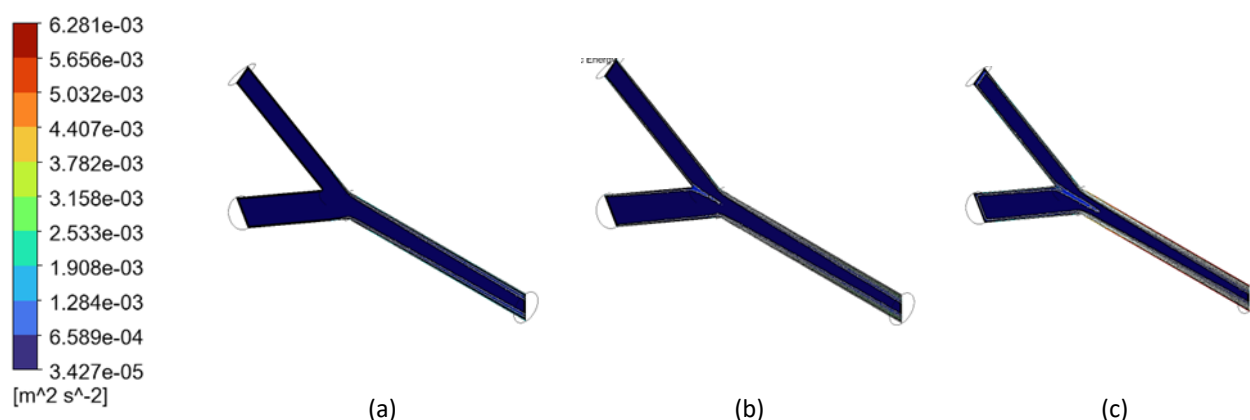


Fig. 8. Turbulence kinetic energy distribution for Y Junction pipe of diameter 0.1 m (a) Inlet velocity = 0.297 m/s (b) Inlet velocity = 0.397 m/s (c) Inlet velocity = 0.497 m/s

In Figure 9(a), the setting depicts the beginning of the story as relatively undisturbed. Dark blue, corresponding to the smallest values of TKE on the colour scale, dominates the entire pipe. There is only an extremely thin pale line of slightly lighter blue tracking along the walls of the pipe, which indicates a certain degree of turbulence close the boundaries where the fluid slides past the circumference of the pipe. The central flow is calm; undisturbed. Continuing from Figure 9(a), we can observe small changes that bring us to image Figure 9(b). The thin boundary layer of turbulent flow along the pipe wall becomes more pronounced and coherent, extending over a longer part of the main pipe, and in fact into the branch pipes. The colour changes slightly toward green in some spots, indicating a mild overrun in turbulent kinetic energy. This implies that under these conditions, the fluid is slightly more active near the sidewalls, at the branching region of the Y-junction.

In Figure 9(c) the turbulence narrative climaxes. The wall-bounded turbulence streak now appears more prominent and stretches the length of the main pipe and both branches. The colours right along this boundary are brighter towards the green and even yellow, indicating that the

turbulent kinetic energy has gone up still further. This means that the fluid is moving around more energetically, especially at the junction and walls, while in the middle of the pipe is relatively calm. In all three instances, one thing becomes apparent: the turbulence is primarily forced to the walls of the pipe and at the junction, but the centre of the pipe stays calm. This behaviour is often observed in piped flows, where turbulence is generated by the wall of the pipe and abrupt changes in direction at junctions.

In short, these results indicate that turbulence is low in the core but higher near the walls and particularly at the bifurcation in a Y-junction 0.2 m diameter pipe. This intensity of the turbulence increases from Figure 9(a) to Figure 9(c), it is likely that such a phenomenon is due to changes in inflow conditions, or inlet velocity. For engineers and designers, this information is vital since it shows where mixing, wear or energy losses are more likely to be, leading to better design and maintenance of piping systems.

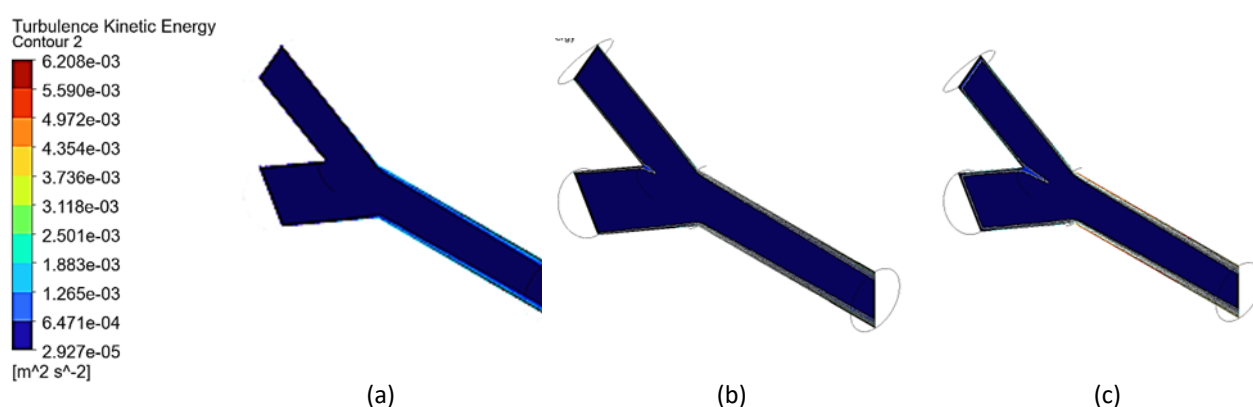


Fig. 9. Turbulence kinetic energy distribution for Y Junction pipe of diameter 0.2 m (a) Inlet velocity = 0.297 m/s (b) Inlet velocity = 0.397 m/s (c) Inlet velocity = 0.497 m/s

3.3.3 Pressure distribution

The solution is presented in Figure 10 and shows the pressure distribution in a Y-shape pipe system with branch and main pipe diameters equal to 0.1 m. The pressure fluctuation is colour coded, in the colormap, the red stands for pressure as high as 519 Pa, while blue as low as -279 Pa. In each of the figure, the highest pressure occurs at the bifurcation (the point where the pipe stems into two branches). This area is always depicted in red/oranges, which implies high-pressure accumulation at the bifurcation. As the flow from these points diverges between the branches, pressure diminishes incrementally. This is mapped from red and orange at the intersection, to green and yellow, and finally to blue at the termini of the conduits, where the pressure is at its lowest.

Each subsection corresponds to a different choice or perspective, yet the general trend persists. This can be observed in Figure 10(a) where pressure distribution is smoother from high to low pressure values. In Figure 10(b), the region of high pressure covers a greater part of the branches, indicating a case with higher input pressure or under different flow conditions. Figure 10(c) presents a pattern like Figure 10(b), but the high-pressure region is not as far-reaching as in Figure 10(b), perhaps because of a different boundary condition or flow rate. Overall, such findings directly show where the pressure flows in the configuration of branching pipe system. The greatest pressures are at the bifurcation at which the flow separates, and the pressure diminishes as the fluid flows along the branches. This behaviour is to be expected for such systems, and it is of particular networking-interest to know where reinforcements in the network should be made and how the fluid will act as it moves through the network.

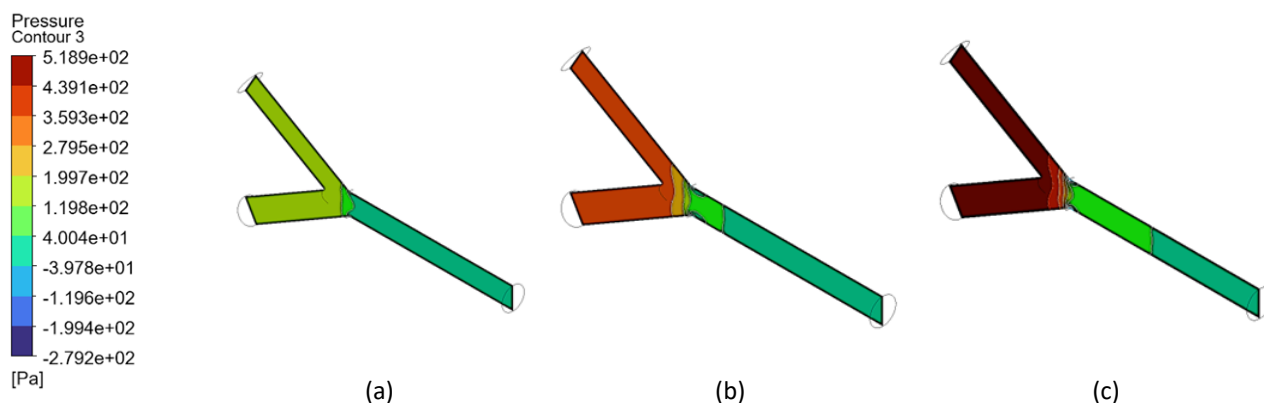


Fig. 10. Pressure distribution for Y Junction pipe of diameter 0.1 m (a) Inlet velocity = 0.297 m/s (b) Inlet velocity = 0.397 m/s (c) Inlet velocity = 0.497 m/s

In Figure 11(a), the high-pressure region is fairly localized at the junction and with moderate smooth drop of pressure on waves propagating along the branches. Figure 11(b) provides a larger area of high pressure which is suggestive of a case of a higher inlet pressure or a change in the flow regime. Figure 11(c) also shows that there is a large high-pressure region at the junction with pressure gradient reaching up further down the main pipe and branches in comparison to Figure 11(a). In general, the results demonstrate the greatest pressure is developed at the bifurcation, followed by a decay and redistribution in the network pipeline. It is a common pattern in branching pipe system and is useful in describing where structural support may be necessary and the behaviour of the fluid flow through the system. Colour contours improve the visualization of such pressure variations and help in the evaluation and design of these piping networks.

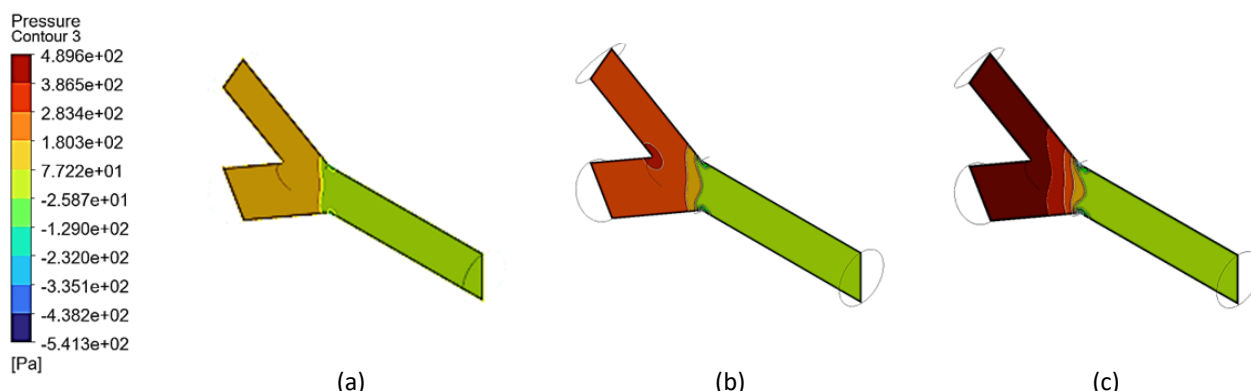


Fig. 11. Pressure distribution for Y Junction pipe of diameter 0.2 m (a) Inlet velocity = 0.297 m/s (b) Inlet velocity = 0.397 m/s (c) Inlet velocity = 0.497 m/s

5. Conclusions

Based on the CFD simulation of the Y-shaped pipeline with two different diameters (0.1 m and 0.2 m), it can be concluded that the pipe diameter has a significant effect on the fluid flow characteristics, namely velocity, turbulence kinetic energy, and pressure distribution. For velocity, the results show that smaller diameter pipes (0.1 m) generate higher flow speeds, especially around the junction and outlet. This is due to the reduced cross-sectional area, which forces the fluid to accelerate. In contrast, the 0.2 m pipe allows for a slower and more uniform velocity profile due to the larger flow area, reducing the overall velocity magnitude. In terms of turbulence, the 0.1 m diameter pipe exhibited higher turbulence kinetic energy, particularly at the Y-junction, indicating

more chaotic and unstable flow behaviours. This is a result of sharper flow redirection in the narrower pipe. The 0.2 m pipe, on the other hand, demonstrated lower turbulence levels, reflecting more stable and smoother fluid motion throughout the pipeline.

Pressure analysis revealed that pressure drops are more significant in the 0.1 m pipe, where a sharp decrease in pressure occurs along the flow direction due to higher velocity and turbulence. Meanwhile, the 0.2m pipe experienced a more gradual and consistent pressure drop, maintaining more stable pressure throughout the pipeline. Finally, increasing the pipeline diameter results in a reduction of flow velocity and turbulence, as well as a more stable pressure distribution. Therefore, for applications requiring stable flow with minimal energy loss and turbulence, a larger diameter Y-pipeline is preferable. However, if higher velocity is desired for specific fluid dynamics, a smaller diameter may be more suitable though with the trade-off of increased turbulence and pressure drop.

References

- [1] Gajbhiye, Bhavesh D., Harshawardhan A. Kulkarni, Shashank S. Tiwari, and Channamallikarjun S. Mathpati. "Teaching turbulent flow through pipe fittings using computational fluid dynamics approach." *Engineering Reports* 2, no. 1 (2020): e12093. <https://doi.org/10.1002/eng2.12093>
- [2] Shao, Yu, Lei Zhao, Y. Jeffrey Yang, Tuqiao Zhang, and Miaomiao Ye. "Experimentally determined solute mixing under laminar and transitional flows at junctions in water distribution systems." *Advances in Civil Engineering* 2019, no. 1 (2019): 3686510, <https://doi.org/10.1155/2019/3686510>
- [3] Lučin, Ivana, Lado Kranjčević, Zoran Čarija, and Antonio Mogorović. "Experimental Setup of Fluid Mixing in Double Tee-Junctions." In *Annals of DAAAM and Proceedings of the International DAAAM Symposium*, p. 1059-1064. Beč: DAAAM International Vienna, 2018. <https://doi.org/10.2507/29th.daaam.proceedings.151>
- [4] Yousef, Khaled, Ahmed Hegazy, and Fatma Saleh. "Numerical Study of Induced Condensation upon Mixing Flows of Water-stream Flow in a Tee-Junction Pipe." *ERJ. Engineering Research Journal* 44, no. 2 (2021): 159-174. <https://doi.org/10.21608/erjm.2021.52289.1056>
- [5] Taha, Enas Salman, Mohammed A. Abdulwahid, Akeel M. Ali Morad, and Qusay A. Maatooq. "Computational fluid dynamic analysis of the flow through T-junction and venturi meter." *IMDC-IST* (2022). <https://doi.org/10.4108/eai.7-9-2021.2314880>
- [6] Ferreira, Ronaldo Novaes, Leonardo Machado Da Rosa, and Johannes Gérson Janzen. "Effect of 90° elbows on pump inlet flow conditions." *Applied Water Science* 10, no. 7 (2020): 1-8. <https://doi.org/10.1007/s13201-020-01255-7>
- [7] Decaix, Jean, Jean-Louis Drommi, François Avellan, and Cécile Münch-Alligné. "CFD simulations of hydraulic short-circuits in junctions, application to the Grand'Maison power plant." In *IOP Conference Series: Earth and Environmental Science*, vol. 1079, no. 1, p. 012106. IOP Publishing, 2022. <https://doi.org/10.1088/1755-1315/1079/1/012106>
- [8] Lopez-Santana, Gabriela, Andrew Kennaugh, and Amir Keshmiri. "Experimental techniques against RANS method in a fully developed turbulent pipe flow: evolution of experimental and computational methods for the study of turbulence." *Fluids* 7, no. 2 (2022): 78. <https://doi.org/10.3390/fluids7020078>
- [9] Vigolo, Daniele, Stefan Radl, and Howard A. Stone. "Unexpected trapping of particles at a T junction." *Proceedings of the National Academy of Sciences* 111, no. 13 (2014): 4770-4775. <https://doi.org/10.1073/pnas.1321585111>
- [10] Doi, Taiga, Takashi Futatsugi, Michio Murase, Kosuke Hayashi, Shigeo Hosokawa, and Akio Tomiyama. "Countercurrent Flow Limitation at the Junction between the Surge Line and the Pressurizer of a PWR." *Science and Technology of Nuclear Installations* 2012, no. 1 (2012): 754724. <https://doi.org/10.1155/2012/754724>
- [11] Marušić-Paloka, Eduard. "Rigorous justification of the Kirchhoff law for junction of thin pipes filled with viscous fluid." *Asymptotic Analysis* 33, no. 1 (2003): 51-66. <https://doi.org/10.3233/ASY-2003-543>
- [12] Decaix, Jean, Mathieu Mettelle, Nicolas Hugo, Bernard Valluy, and Cécile Münch-Alligné. "CFD investigation of the hydraulic short-circuit mode in the FMHL/FMHL+ pumped storage power plant." *Energies* 17, no. 2 (2024): 473. <https://doi.org/10.3390/en17020473>
- [13] Ando, Toshitake, Toshihiko Shakouchi, Satoru Takamura, and Koichi Tsujimoto. "Effects of flow rate ratio on loss reduction of T-junction pipe." *Journal of Fluid Science and Technology* 9, no. 3 (2014): JFST0045-JFST0045. <https://doi.org/10.1299/jfst.2014jfst0045>
- [14] Raschi, Marcelo, Fernando Mut, Greg Byrne, Christopher M. Putman, Satoshi Tateshima, Fernando Viñuela, Tetsuya Tanoue, Kazuo Tanishita, and Juan R. Cebal. "CFD and PIV analysis of hemodynamics in a growing intracranial aneurysm." *International Journal for Numerical Methods in Biomedical Engineering* 28, no. 2 (2012): 214-228. <https://doi.org/10.1002/cnm.1459>

- [15] Hoi, Yiemeng, Scott H. Woodward, Minsuok Kim, Dale B. Taulbee, and Hui Meng. "Validation of CFD simulations of cerebral aneurysms with implication of geometric variations." (2006): 844-851. <https://doi.org/10.1115/1.2354209>
- [16] Miyazaki, Shohei, Keiichi Itatani, Toyoki Furusawa, Teruyasu Nishino, Masataka Sugiyama, Yasuo Takehara, and Satoshi Yasukochi. "Validation of numerical simulation methods in aortic arch using 4D Flow MRI." *Heart and vessels* 32, no. 8 (2017): 1032-1044. <https://doi.org/10.1007/s00380-017-0979-2>
- [17] Hardy, R. J., S. N. Lane, and D. Yu. "Flow structures at an idealized bifurcation: a numerical experiment." *Earth Surface Processes and Landforms* 36, no. 15 (2011): 2083-2096, <https://doi.org/10.1002/esp.2235>
- [18] Zhang, Xiang, Genglei Xia, Tenglong Cong, Minjun Peng, and Zhenhong Wang. "Uncertainty analysis on k- ϵ turbulence model in the prediction of subcooled boiling in vertical pipes." *Frontiers in Energy Research* 8 (2020): 584531, <https://doi.org/10.3389/fenrg.2020.584531>
- [19] Yin, Jun-Lian, De-Zhong Wang, Yu-Lin Wu, and D. Keith Walters. "A modified k- ϵ model for computation of flows with large streamline curvature." *Advances in Mechanical Engineering* 5 (2013): 592420. <https://doi.org/10.1155/2013/592420>
- [20] Boz, Ziyinet, Ferruh Erdogan, and Mustafa Tutar. "Effects of mesh refinement, time step size and numerical scheme on the computational modeling of temperature evolution during natural-convection heating." *Journal of Food Engineering* 123 (2014): 8-16, <https://doi.org/10.1016/j.jfoodeng.2013.09.008>